

web page: <http://w3.pppl.gov/~zakharov>

The theory of variances of equilibrium current density reconstruction¹

Leonid E. Zakharov, Jerome Lewandowski

Princeton Plasma Physics Laboratory, MS-27 P.O. Box 451, Princeton NJ 08543-0451

Vladimir Drozdov, Darren McDonald

EURATOM/UKAEA Fusion Association, Culham Science Centre, Abingdon, OXON, OX14 3DB UK

EFDA-JET Seminar

July 28, 2006, Culham Science Center, Culham, UK

¹ This work is supported by US DoE contract No. DE-AC020-76-CHO-3073.

Abstract

The talk presents a rigorous theory of uncertainties in the reconstructions of the plasma current density and pressure profiles in the Grad-Shafranov equation. The associated technique was incorporated into the ESC code, which provides the calculations of characteristic cases with different plasma cross-sections, aspect ratios and current distributions.

Contents

| | | |
|----------|-------------------------------------------------------------------------------------------|-----------|
| 1 | A “rigorous” theory for a “non-rigorous” reality | 4 |
| 1.1 | <i>Linearized Grad-Shafranov equation</i> | 5 |
| 1.2 | <i>Singular Value Decomposition (SVD) and variances in \bar{j}</i> | 8 |
| 2 | Characteristic cases of tokamak equilibria | 11 |
| 2.1 | <i>Shafranov’s model of circular cross-section</i> | 12 |
| 2.2 | <i>Equilibrium with a circular cross-section</i> | 13 |
| 2.3 | <i>Non-circular cross-sections</i> | 17 |
| 2.4 | <i>Spherical tokamaks</i> | 20 |
| 3 | Summary | 25 |

1 A “rigorous” theory for a “non-rigorous” reality

The first reconstruction was motivated by experimentalists (A.Bortnikov)

eld measured along a ... the current. The distribu-
tion of the tangenti **1973** B_θ along the contour is give

Moscow Conf. on Pl.Ph. & Cntr.Fs.

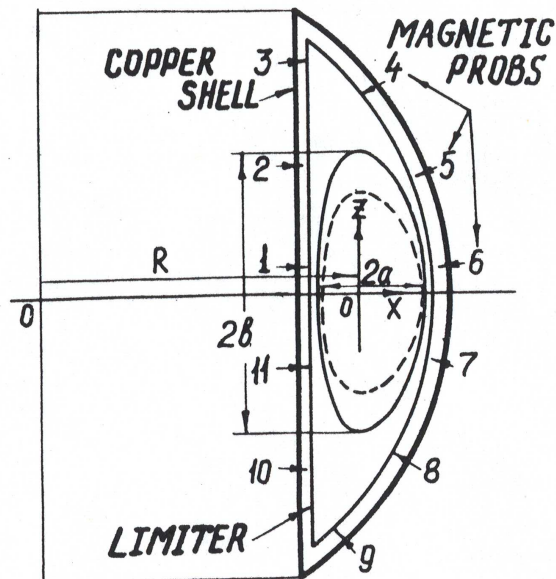


Fig. 3.

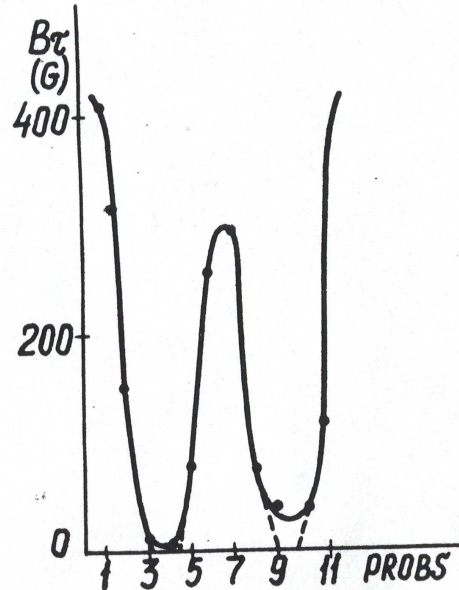


Fig. 4.

$$\Delta^* \bar{\Psi} = -J(r, \bar{\Psi})$$

T-9 (finger-ring tokamak) Kurchatov

The HDG (Hand Driven Graphics) did prove the existence of elongation

Basic notations for the Grad-Shafranov (GSh) equation

$$\begin{aligned}
 \Delta^* \bar{\Psi} &\equiv \frac{\partial^2 \bar{\Psi}}{\partial r^2} - \frac{1}{r} \frac{\partial \bar{\Psi}}{\partial r} + \frac{\partial^2 \bar{\Psi}}{\partial z^2} = -T - r^2 P, \quad \bar{\Psi} \equiv \frac{\Psi}{2\pi}, \\
 T = T(\bar{\Psi}) &\equiv \bar{F} \frac{d\bar{F}}{d\bar{\Psi}}, \quad \bar{F} \equiv r B_\varphi, \\
 P = P(\bar{\Psi}) &\equiv \bar{p}', \\
 \mathbf{B} = \mathbf{B}_{pol} + \frac{1}{r} \bar{F}(\bar{\Psi}) \mathbf{e}_\varphi, \quad \mathbf{B}_{pol} &= \frac{1}{r} (\nabla \bar{\Psi} \times \mathbf{e}_\varphi), \\
 \bar{p} = \mu_0 p(\bar{\Psi}), \quad \bar{j}(r, \bar{\Psi}) &\equiv \mu_0 j_\varphi = \frac{1}{r} T + r P
 \end{aligned} \tag{1.1}$$

GSh equation requires the boundary conditions and $T(\bar{\Psi})$, $P(\bar{\Psi})$

Linearization is the fastest method of solving GSh equation

In flux coordinates a, φ, θ

$$\begin{aligned}\Delta^* \bar{\Psi} &= -T(\bar{\Psi}) - r^2 P(\bar{\Psi}), \quad \bar{\Psi} = \bar{\Psi}_0(a) + \psi(a, \theta), \\ \Delta^* \bar{\Psi} &= -T(\bar{\Psi}_0) - r^2 P(\bar{\Psi}_0) - \frac{dT(\bar{\Psi}_0)}{d\bar{\Psi}_0} \psi - r^2 \frac{dP(\bar{\Psi}_0)}{d\bar{\Psi}_0} \psi, \\ \Delta^* \bar{\Psi}_0 &= -T - r^2 P, \quad \Delta^* \psi + T' \psi + r^2 P' \psi = 0, \\ \psi(a, \theta) &\rightarrow \xi(a, \theta) = -\frac{\psi(a, \theta)}{\bar{\Psi}'_0}, \\ r(a + \xi, \theta) &= r(a, \theta) + r'_a \xi, \quad z(a + \xi, \theta) = z(a, \theta) + z'_a \xi\end{aligned}\tag{1.2}$$

As a result of iterations (for given boundary conditions)

$$\psi \rightarrow 0, \quad \bar{\Psi} \rightarrow \bar{\Psi}_0(a)\tag{1.3}$$

This scheme automatically contains the linear response $\xi(a, \theta)$ to possible perturbations of the plasma shape

Measurements of $\bar{\Psi}(r, z)$ and $B_r(r, z)$, $B_z(r, z)$ are “excessive”

They are used to determine the current density of the GSh equation

$$\bar{j}_\varphi \equiv \bar{j}_s(a) \frac{R_0}{r} + \bar{j}_p(a) \left(\frac{r}{R_0} - \frac{R_0}{r} \right), \quad P = \frac{\bar{j}_p}{R_0}, \quad T = R_0(\bar{j}_s - \bar{j}_p), \quad (1.4)$$

$$\bar{j}_s = \bar{j}_{s0} + \sum_{m=0}^{m < N_J} J_m f^m(a), \quad \bar{j}_p = \bar{j}_{p0} + \sum_{m=0}^{m < N_P} P_m f^m(a),$$

where R_0 is the radius of the magnetic axis.

The linear response to perturbation of the current density profile is determined by

$$\Delta^* \bar{\Psi} = -T - r^2 P,$$

$$\Delta^* \psi + T'(\bar{\Psi}) \psi + r^2 P'(\bar{\Psi}) \psi = -R_0 \sum_{m=0}^{m < N_J} J_m f^m(a) \quad (1.5)$$

$$-r \left(\frac{r}{R_0} - \frac{R_0}{r} \right) \sum_{m=0}^{m < N_P} P_m f^m(a)$$

Solving nonlinear GSh equation and perturbation analysis are separated

Perturbations of equilibria perturb the “measurements”

Vectors of perturbations in equilibrium \vec{X} and in measurements $\delta\vec{S}$

$$\xi = \sum_{m=0}^{m < N_b} A_m \xi^m(a, \theta), \quad \delta \bar{j}_s = \sum_{m=0}^{m < N_J} J_m f^m(a), \quad \delta \bar{j}_p = \sum_{m=0}^{m < N_P} P_m f^m(a),$$

$$\vec{X} \equiv \begin{pmatrix} A_0 \\ A_1 \\ \dots \\ A_{N_b-1} \\ J_0 \\ \dots \\ J_{N_J-1} \\ P_0 \\ \dots \\ P_{N_P-1} \end{pmatrix}, \quad \delta \vec{S} \equiv \begin{pmatrix} \Psi_0 \\ \Psi_1 \\ \dots \\ \Psi_{M_\Psi-1} \\ B_0 \\ B_1 \\ \dots \\ B_{M_B-1} \end{pmatrix},$$

$$N \equiv N_b + N_J + N_P$$

$$M \equiv M_\Psi + M_B$$

$$M > N$$

(1.6)

Vectors \vec{X} and $\delta\vec{S}$ are linearly related

Linearized GSh equation determines the response matrix \mathbf{A}

$$\mathbf{A}\vec{X} = \delta\vec{S}, \quad \mathbf{A} = \mathbf{A}_{M \times N} \quad (1.7)$$

Using the SVD technique, \mathbf{A} can be expressed as a product

$$\mathbf{A} = \mathbf{U} \cdot \mathbf{W} \cdot \mathbf{V}^T,$$
$$\mathbf{U} = \mathbf{U}_{M \times N}, \quad \mathbf{U}^T \cdot \mathbf{U} = \mathbf{I}, \quad I_i^k = \delta_i^k, \quad (1.8)$$

$$\mathbf{W} = \mathbf{W}_{N \times N}, \quad W_i^k = w_i \delta_i^k,$$

$$\mathbf{V} = \mathbf{V}_{N \times N}, \quad \mathbf{V}^T \cdot \mathbf{V} = \mathbf{I}$$

and the solution to it as a linear combination of eigenvectors

$$\vec{X} = \mathbf{V} \cdot \vec{C}, \quad (1.9)$$

where

Columns of \mathbf{V} and w_k represent eigenvectors and eigenvalues

SVD gives a comprehensive information on variances in equilibrium

The contribution of a single eigenvector \vec{X}_k (one column of maV) is determined simply by

$$\vec{X}_k = (\mathbf{V})_k, \quad \delta \vec{S}_k = w_k \vec{U}_k, \quad \vec{U}_k = (\mathbf{U})_k, \quad (1.10)$$

$$(\vec{X}_k^T \cdot \vec{X}_k) = 1, \quad (\vec{U}_k^T \cdot \vec{U}_k) = 1.$$

The eigenvectors \vec{X} and w_k can be renormalized in order to make the perturbations in the current density comparable to the background \bar{j}

$$\mathbf{A} \vec{X}_k = w_k \vec{U}_k,$$

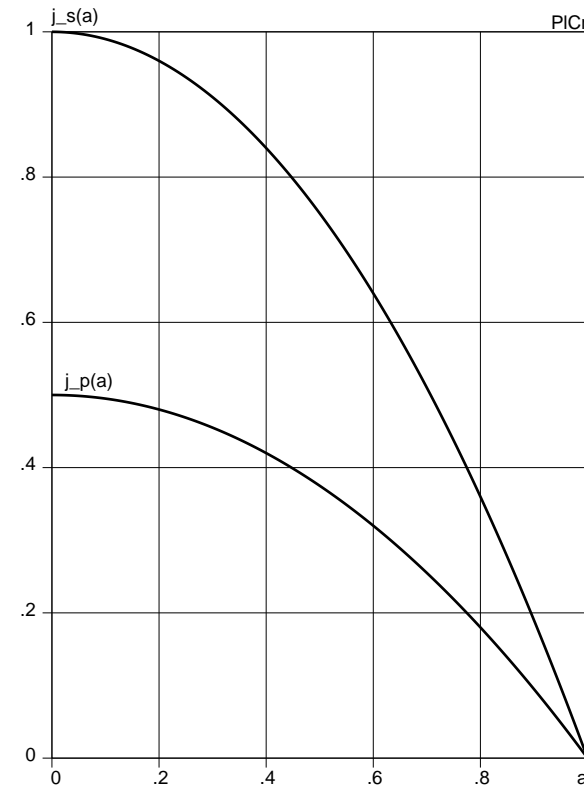
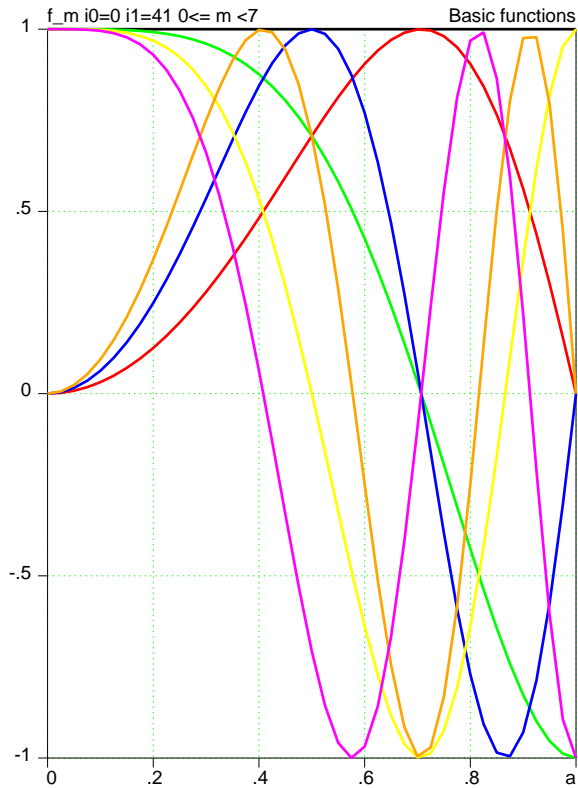
$$\vec{X}_k \rightarrow \alpha \vec{X}_k, \quad w_k \rightarrow \alpha w_k, \quad (1.11)$$

$$\max(\delta \bar{j}_{sk}, \delta \bar{j}_{pk}) = \max(\bar{j}_{sk}, \bar{j}_{pk}).$$

In the following, the perturbations in the plasma shape are dropped

2 Characteristic cases of tokamak equilibria

SVD perturbation analysis can be performed on any given equilibrium



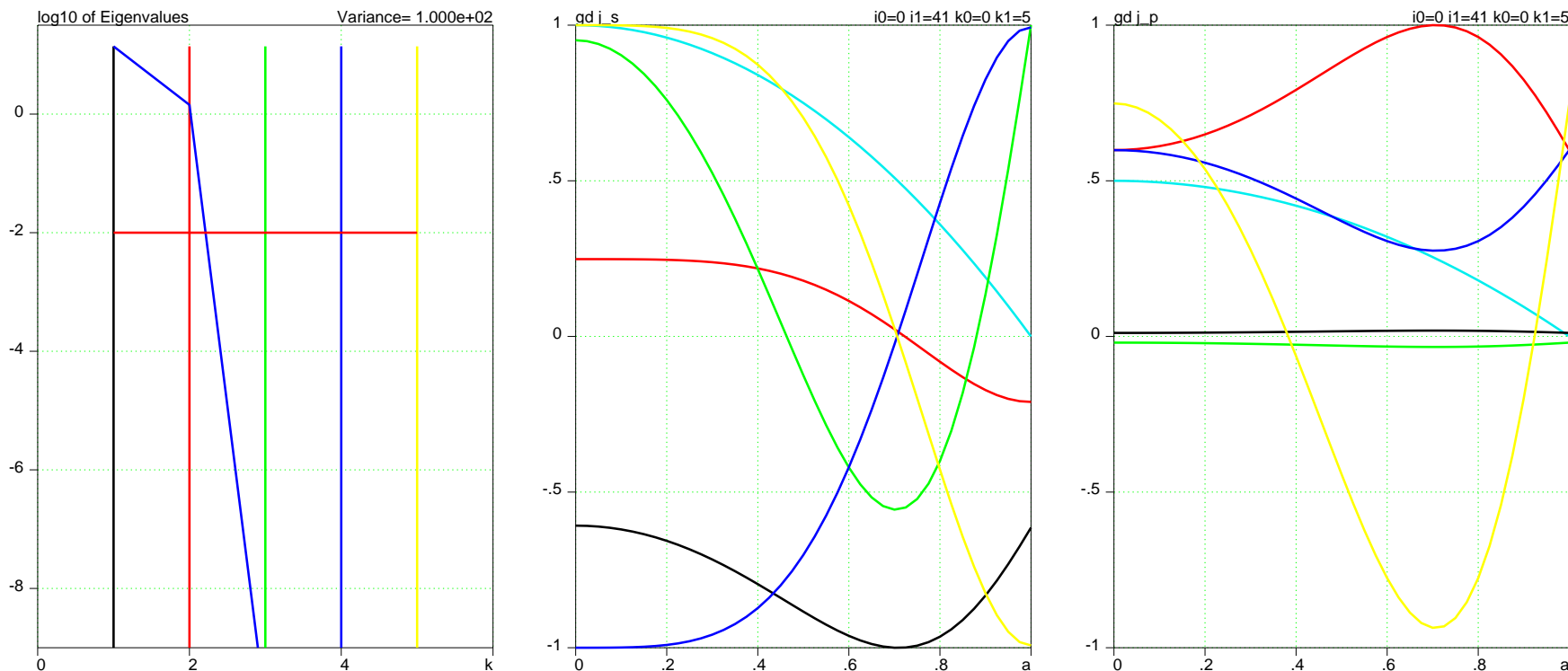
Trigonometric expansion functions

background current density profiles
 $\bar{j}_s(a), \bar{j}_p(a)$

Diamagnetic signal is not taken into account yet

2.1 Shafranov's model of circular cross-section

The model contains only two Fourier harmonics in magnetic geometry

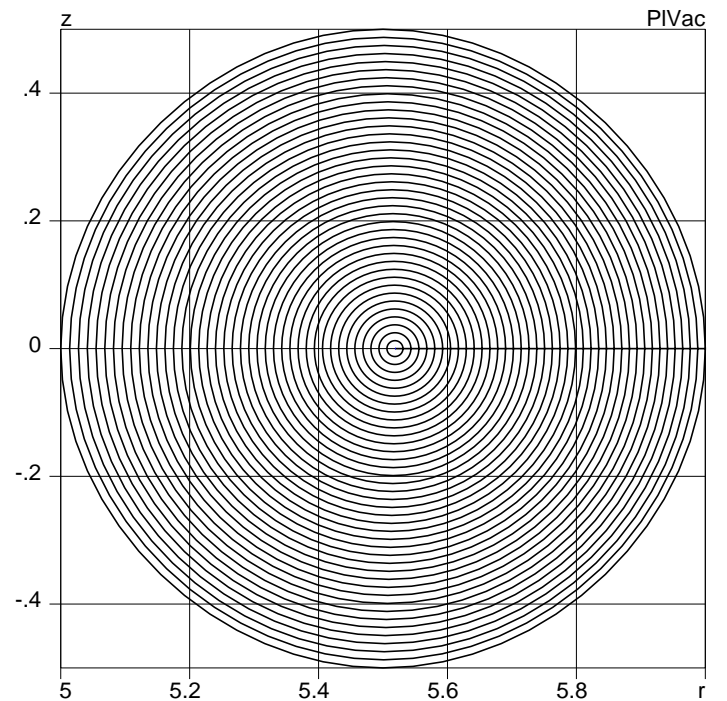


Logarithm of eigen- Eigen-functions $\delta j_s^k(a)$ Eigen-functions $\delta j_p^k(a)$ values w_k ($N_J=3$, $N_P=2$) as functions of a .

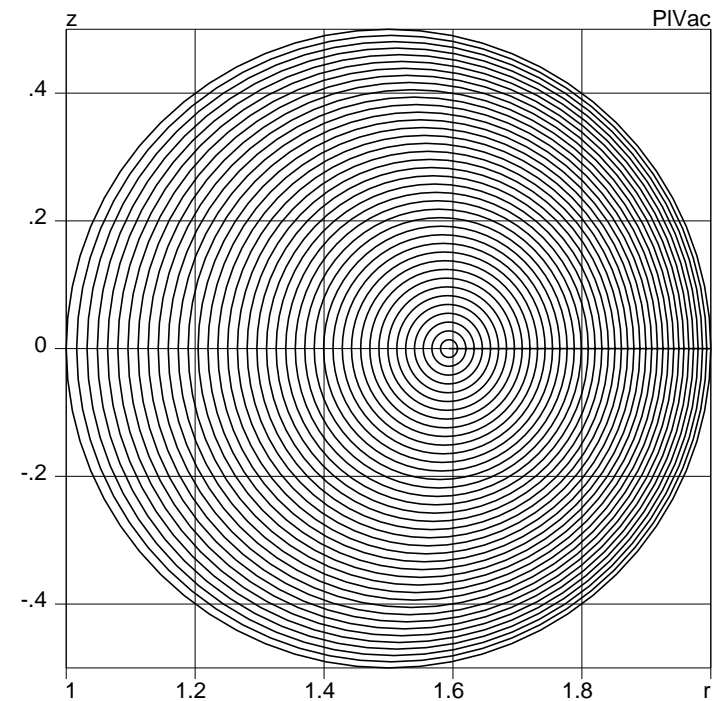
Only two numbers can be determined from external measurements

2.2 Equilibrium with a circular cross-section

Circular equilibria with a full set of Fourier harmonics

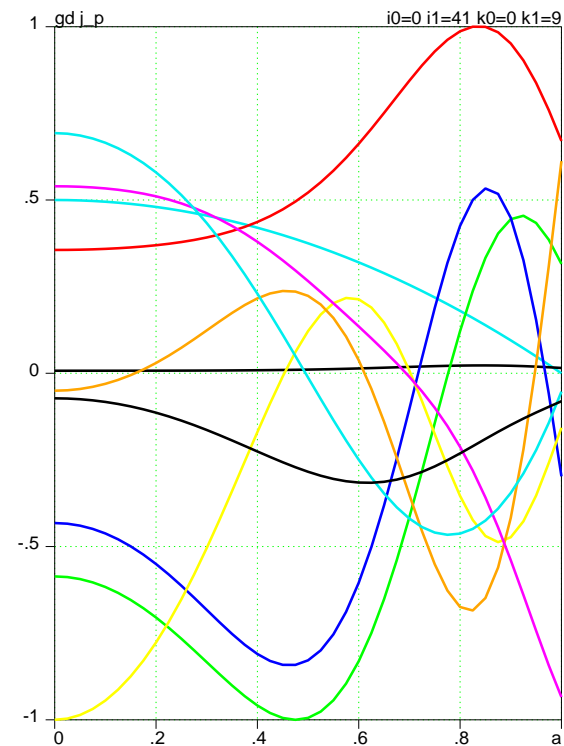
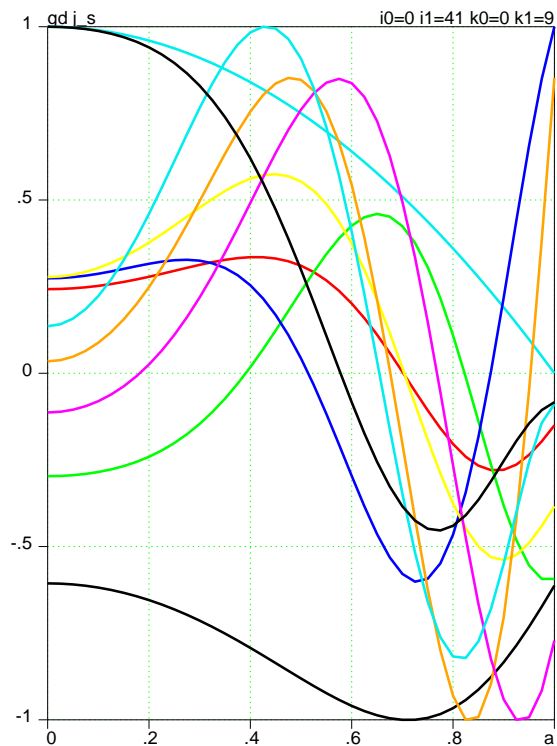
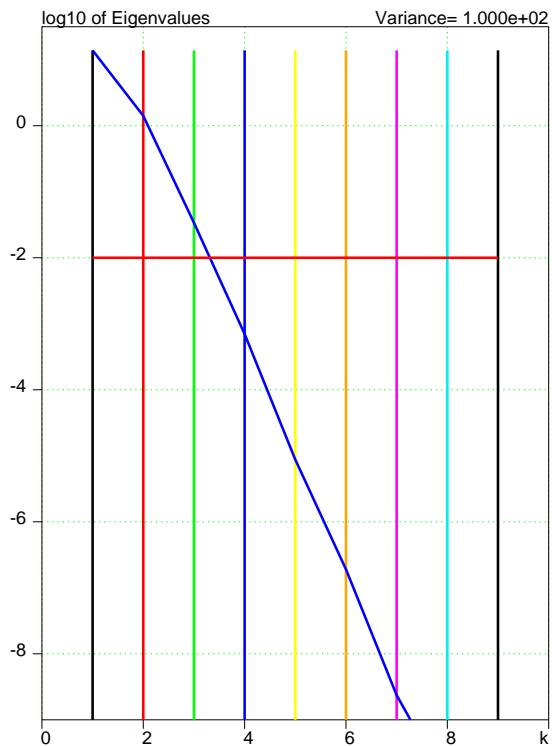


Large $R/a_0 = 10$ aspect ratio.



Medium $R/a_0 = 2$ aspect ratio equilibrium.

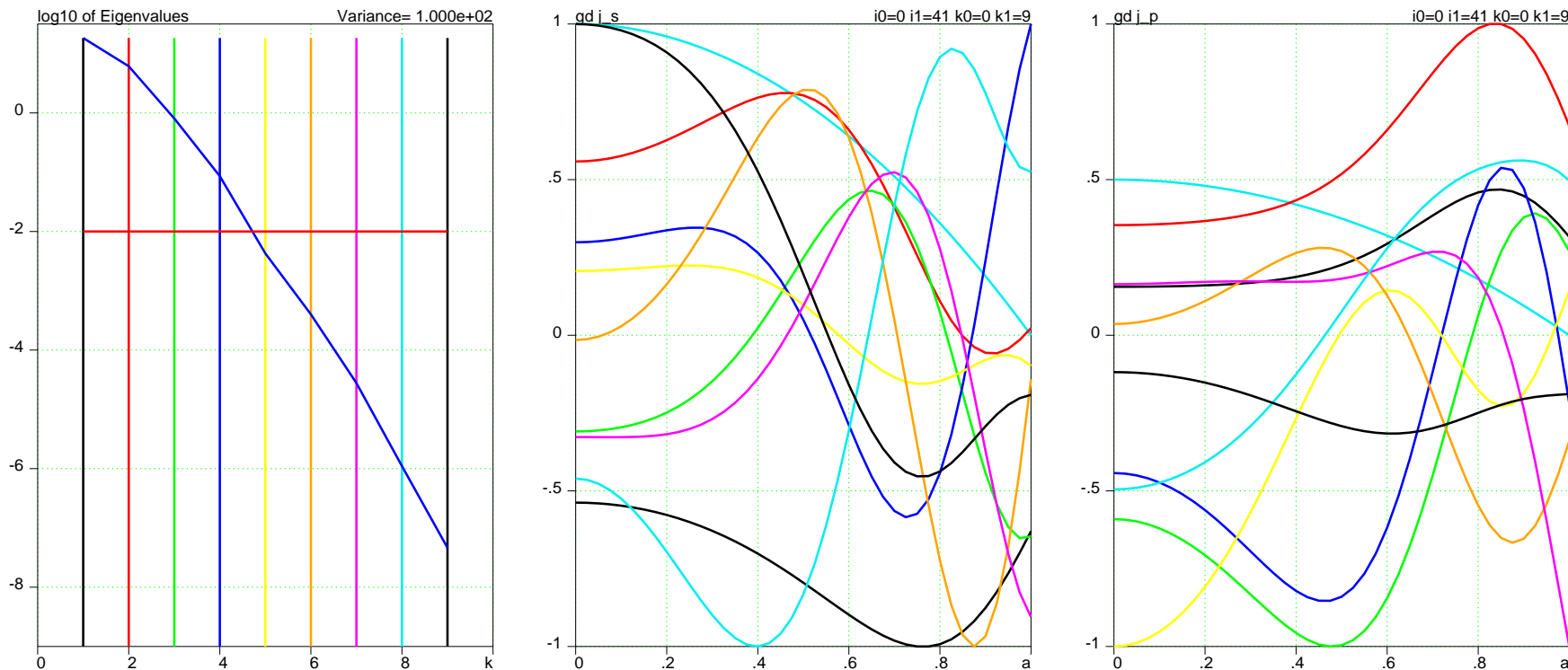
Circular equilibrium for $R/a=10$ is similar to Shafranov's case



Logarithm of eigen-values w_k ($N_J=5$, $N_P=4$) as functions of α . Eigen-functions $\delta j_s^k(a)$ Eigen-functions $\delta j_p^k(a)$

Perturbations with $k > 3$ are invisible on B signals

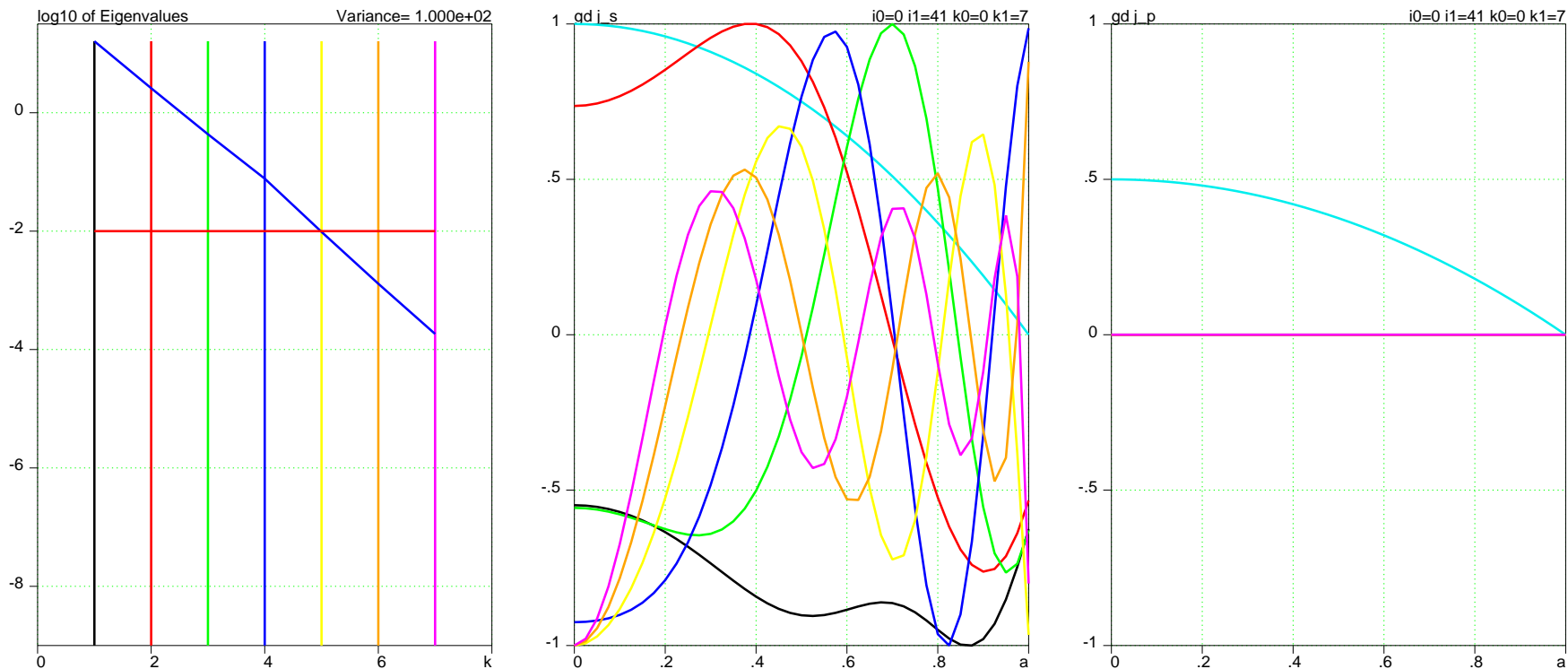
Medium aspect ($R/a=2$) ratio equilibrium. No information on pressure



Logarithm of eigen- Eigen-functions $\delta j_s^k(a)$ Eigen-functions $\delta j_p^k(a)$ values w_k ($N_J=5$, $N_P=4$) as functions of a .

Perturbations with $k > 4$ are invisible on B signals independent on R/a

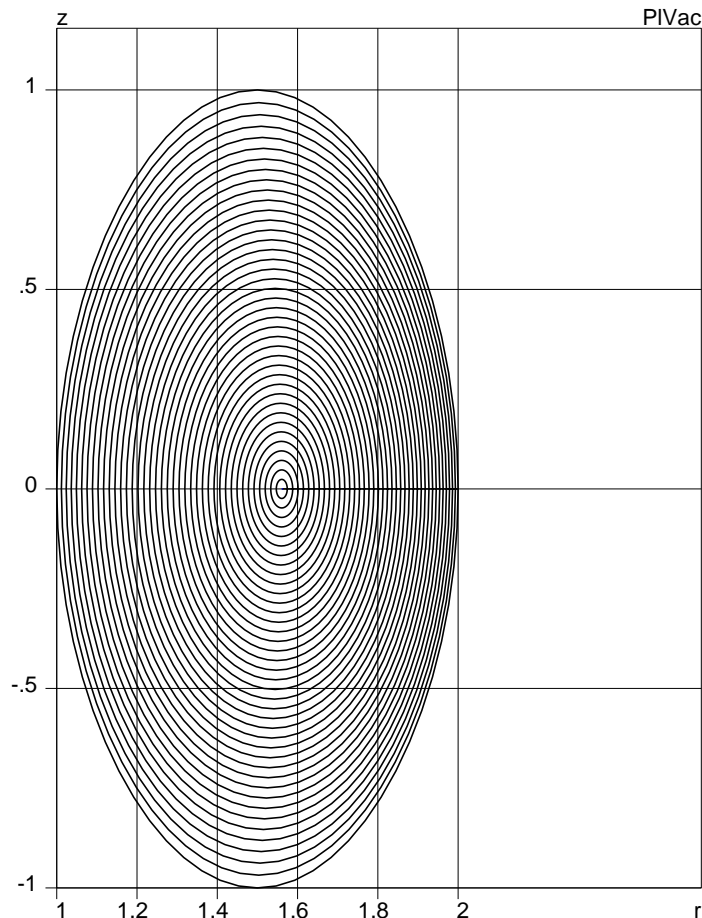
Medium aspect ($R/a=2$) ratio equilibrium. Pressure profile is known



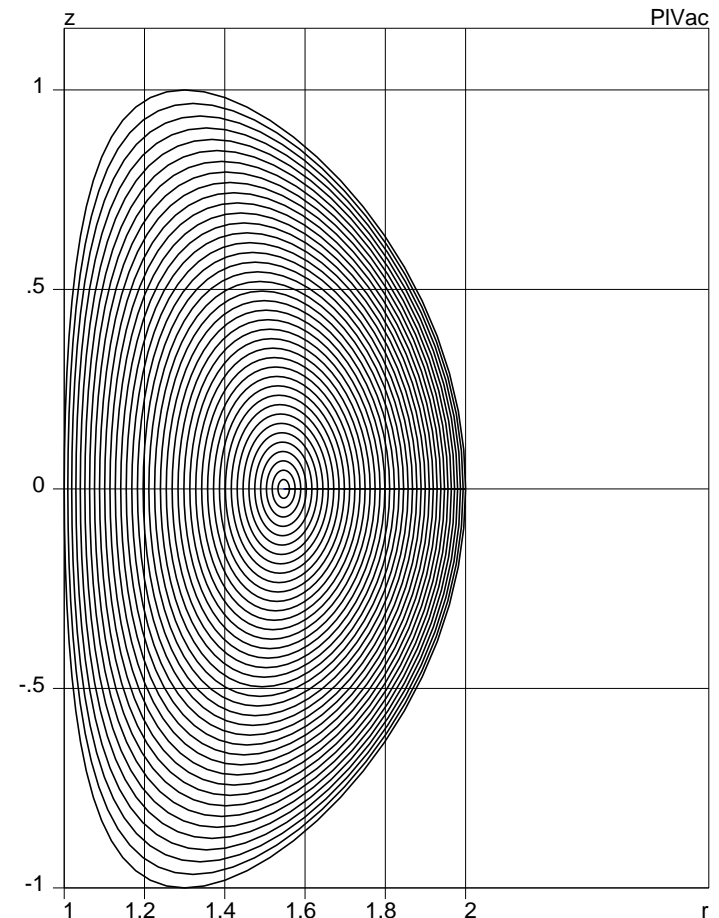
Logarithm of eigen- Eigen-functions $\delta j_s^k(a)$ Eigen-functions $\delta j_p^k(a)$ values w_k ($N_J=7$, $N_P=0$) as functions of a .

Oscillatory perturbations of j_s with $k > 4$ are invisible on B

Pure elliptic $\kappa = 2$ and shaped $\delta = 0.4$ plasma cross-section ($R/a_0=3$)

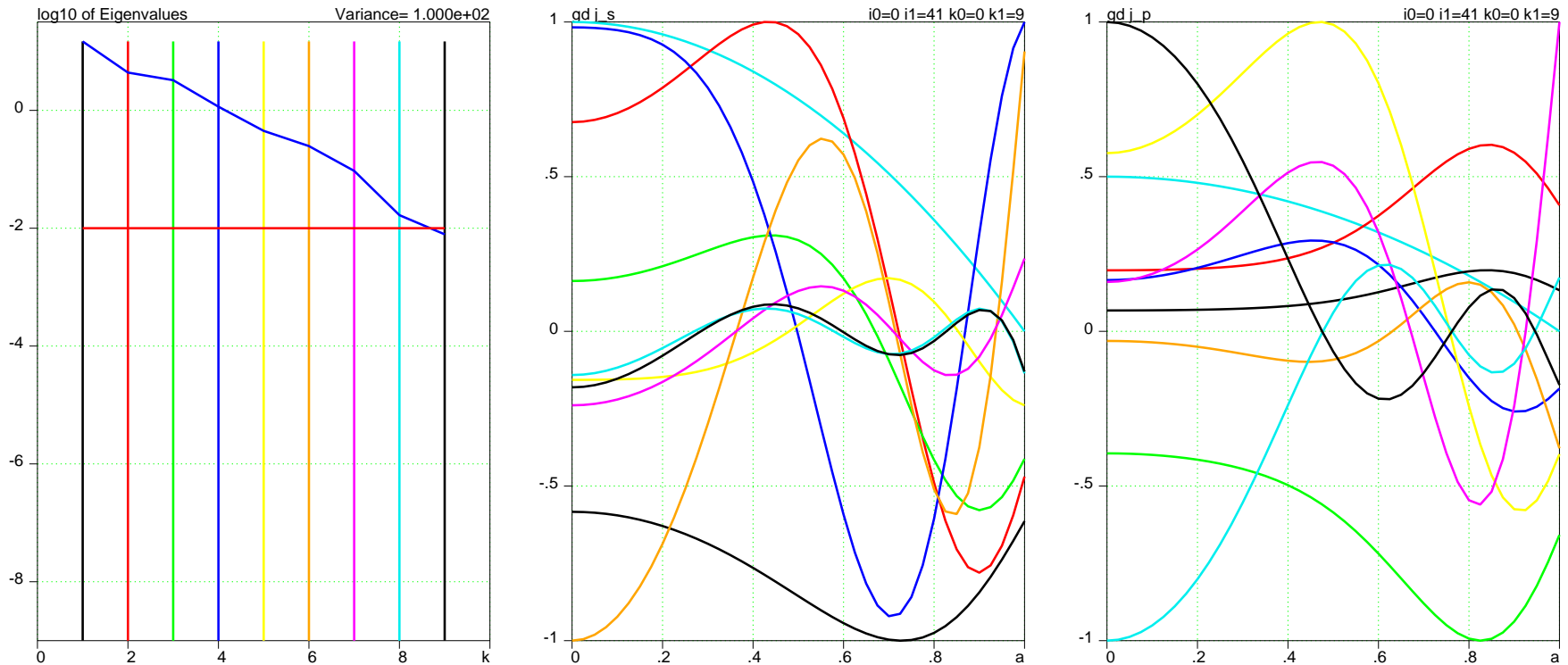


Elliptic plasma, $R/a_0 = 3$



Shaped plasma, $R/a_0 = 3$

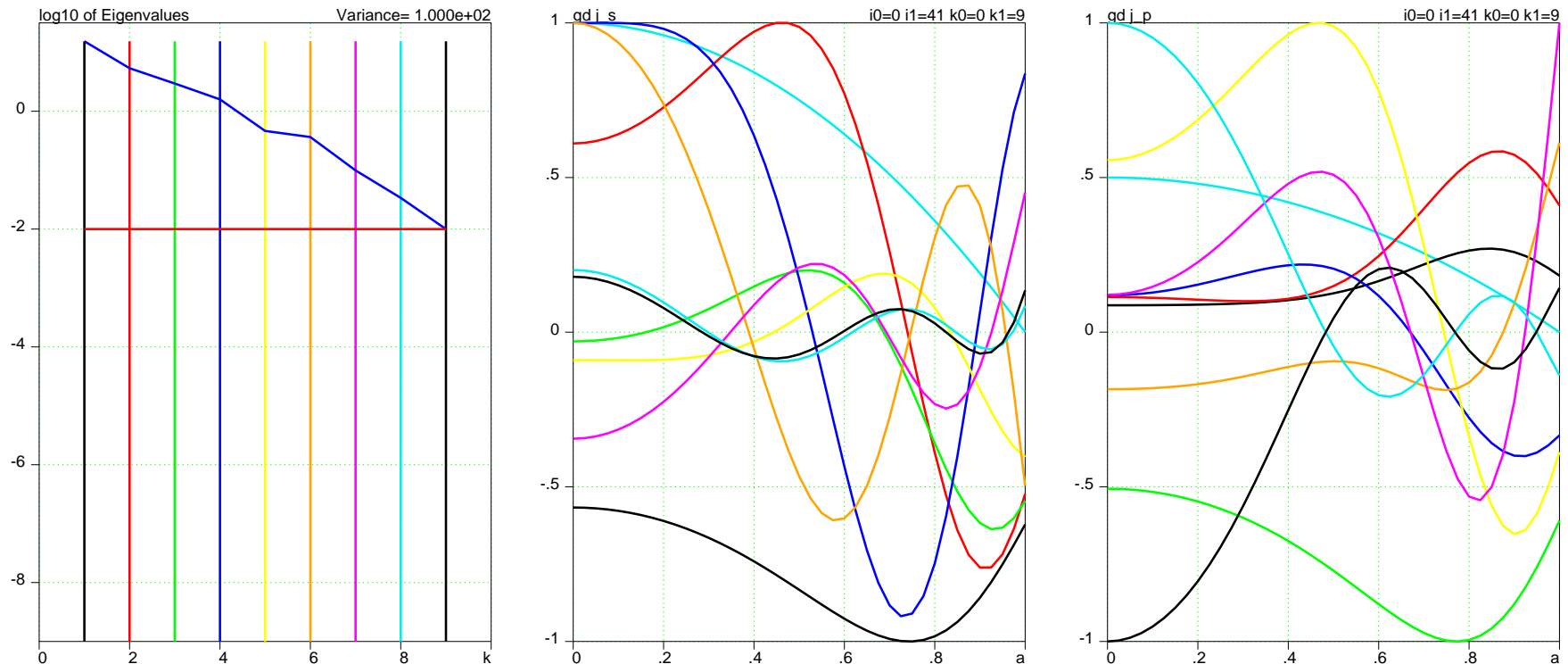
Elliptic plasma shape equilibrium with $R/a=3$. No information on pressure



Logarithm of eigen- Eigen-functions $\delta j_s^k(a)$ Eigen-functions $\delta j_p^k(a)$ values w_k ($N_J=5$, $N_P=4$) as functions of a .

Perturbations with $k > 7$ are invisible on B , j_p cannot be reconstructed

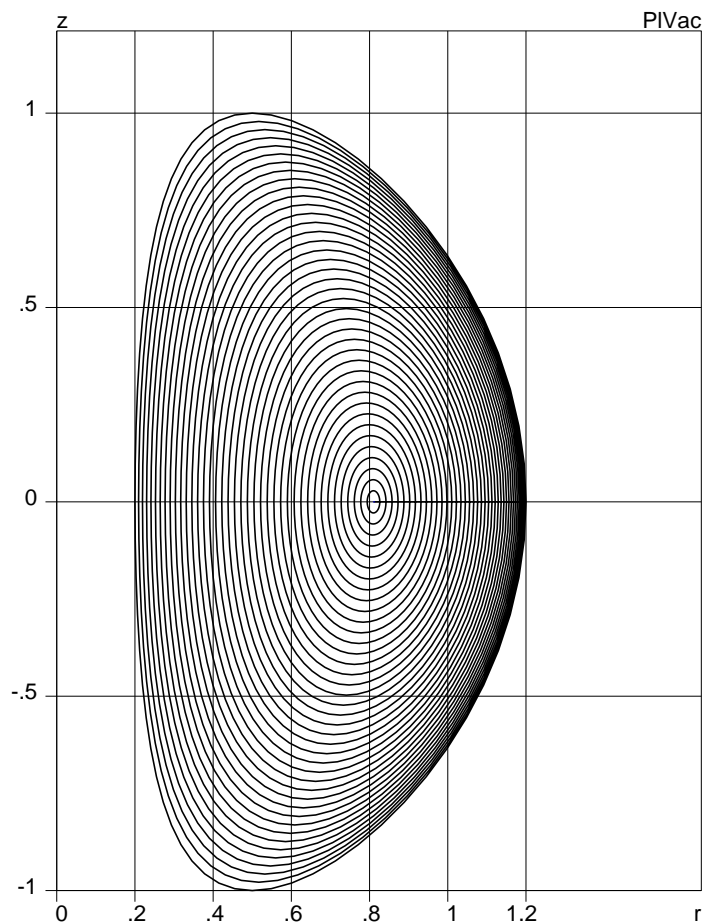
Shaped plasma equilibrium with $R/a=3$. No information on pressure



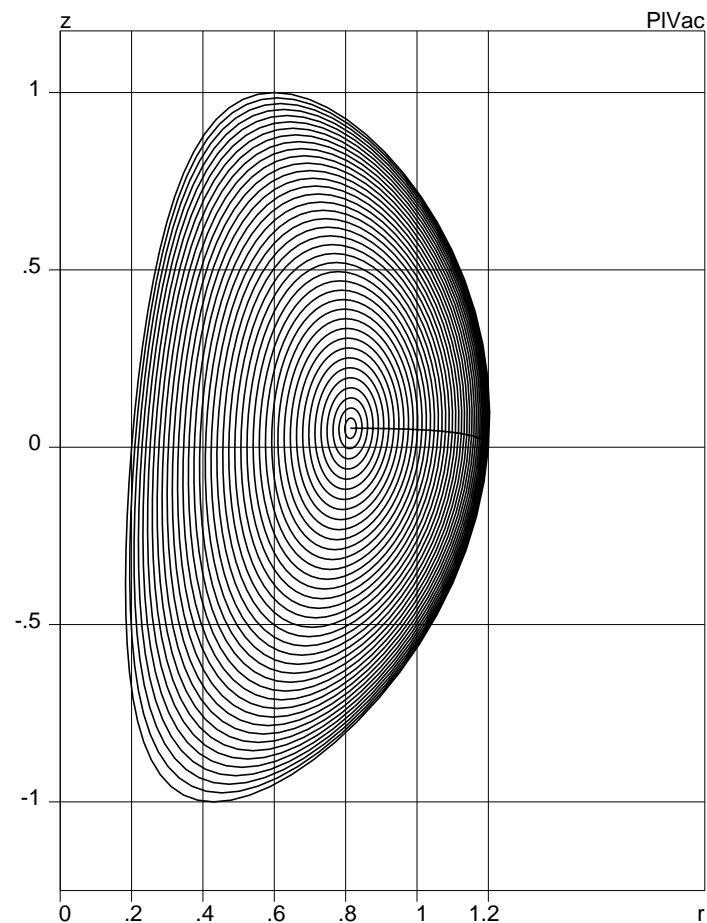
Logarithm of eigen- Eigen-functions $\delta j_s^k(a)$ Eigen-functions $\delta j_p^k(a)$ values w_k ($N_J=5$, $N_P=4$) as functions of a .

Perturbations with $k > 8$ are invisible on B , j_p cannot be reconstructed

Spherical Tokamak equilibria ($R/a=1.4$)

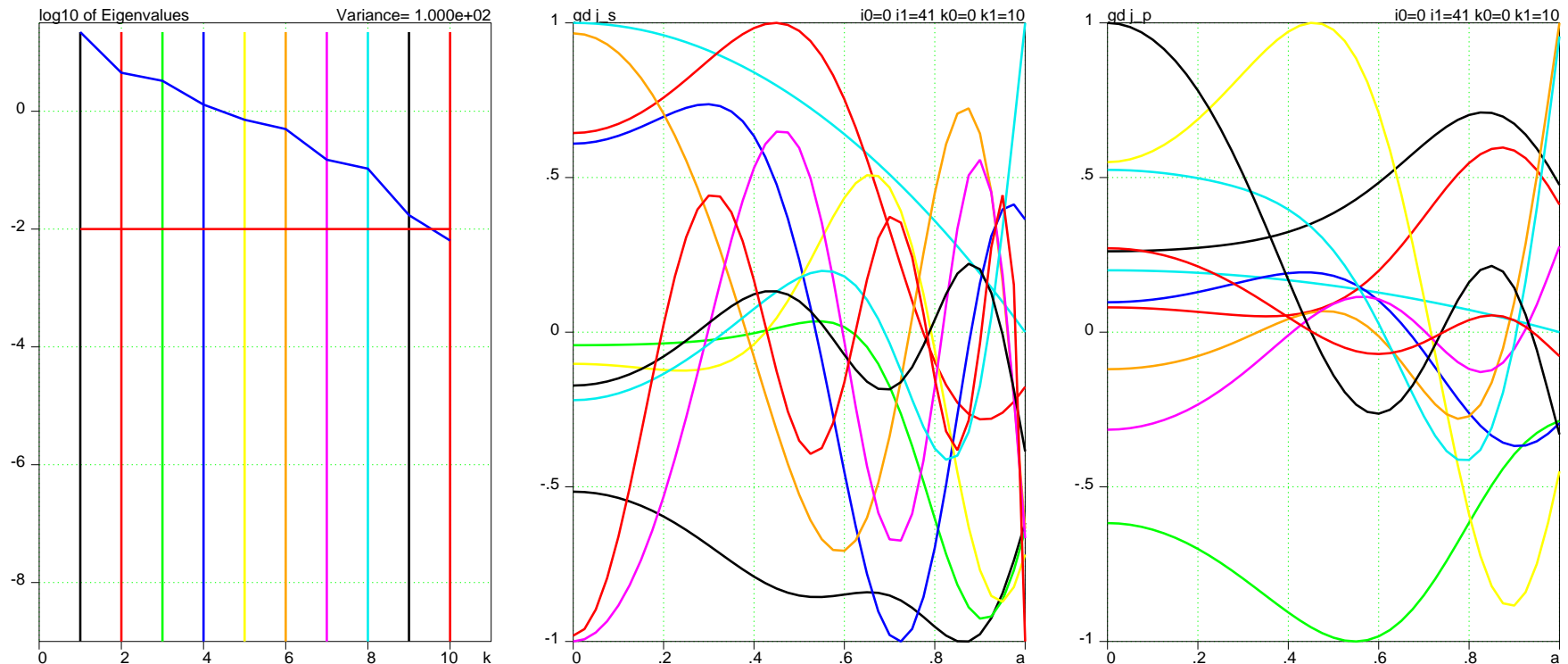


ST-like plasma, $R/a_0 = 1.4$



Slant ST plasma, $R/a_0 = 1.4$

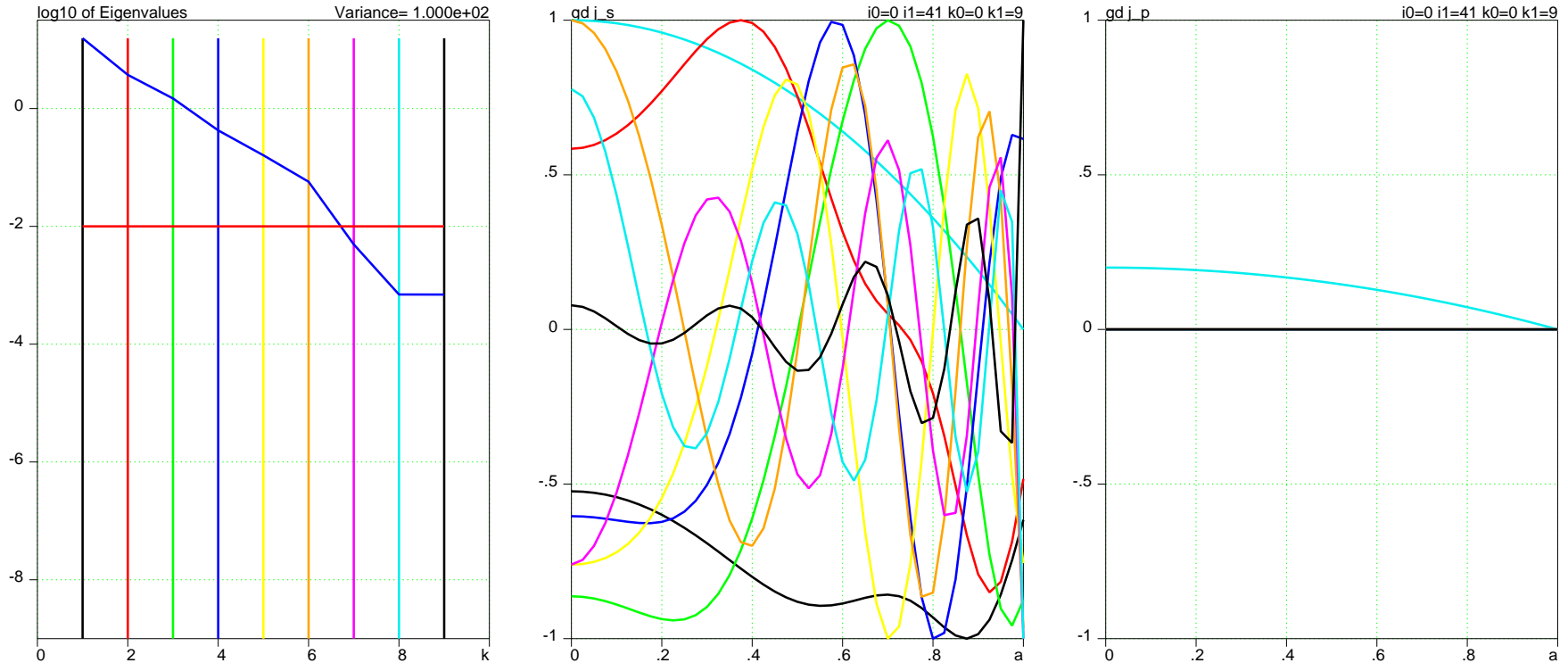
ST-like plasma with $R/a=1.4$. No information on pressure



Logarithm of eigen- Eigen-functions $\delta j_s^k(a)$ Eigen-functions $\delta j_p^k(a)$ values w_k ($N_J=6$, $N_P=4$) as functions of a .

Perturbations with $k > 8$ are invisible on B , j_p cannot be reconstructed

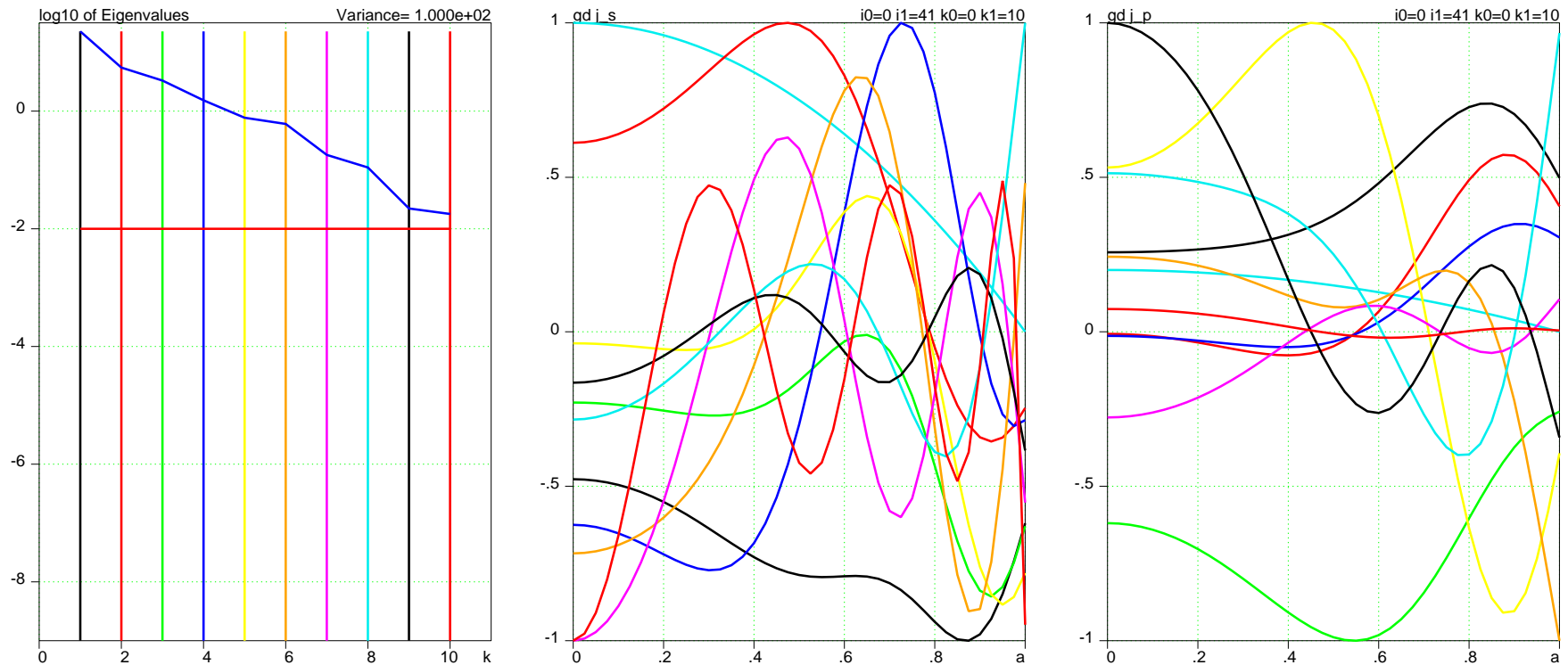
ST-like plasma with $R/a=1.4$. Pressure profile is known



Logarithm of eigen- Eigen-functions $\delta j_s^k(a)$ Eigen-functions $\delta j_p^k(a)$ values w_k ($N_J=9$, $N_P=0$) as functions of a .

Oscillatory perturbations with $k > 6$ are invisible on B

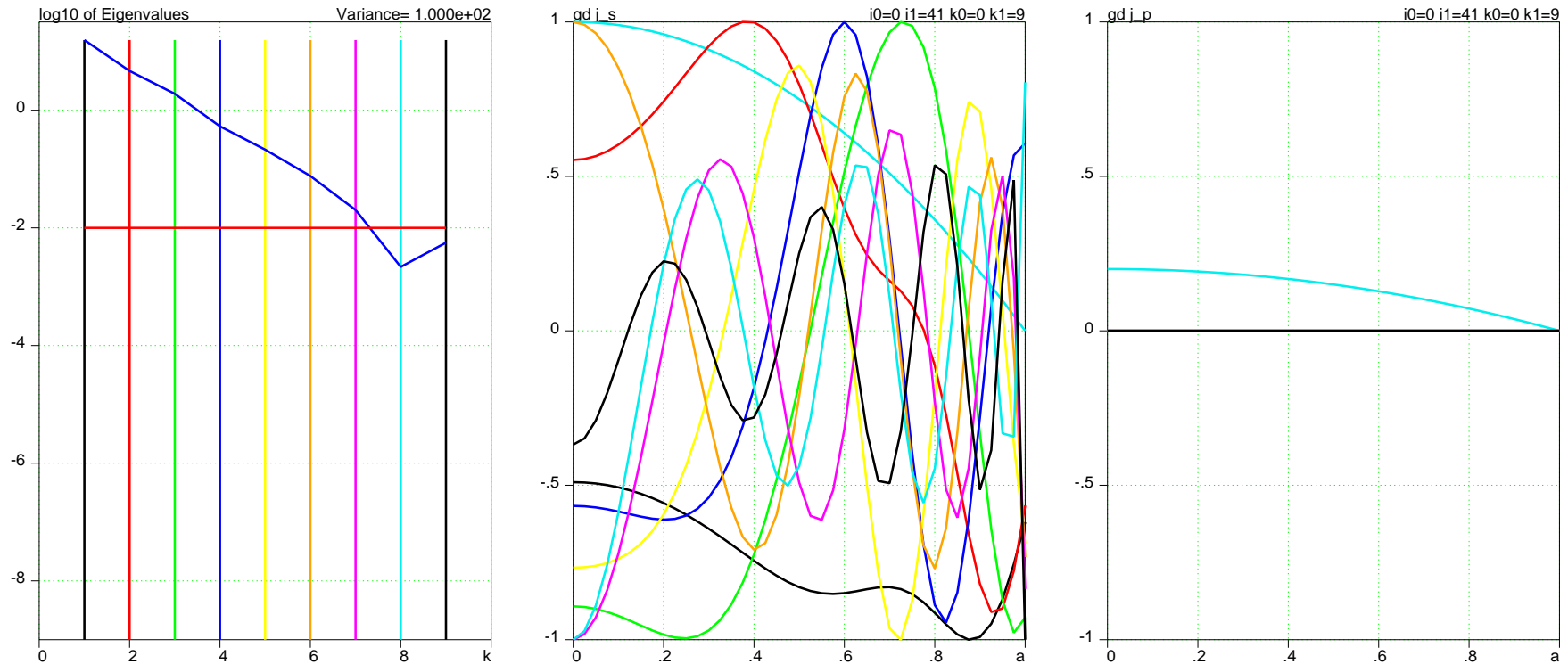
Slant ST plasma with $R/a=1.4$. No information on pressure



Logarithm of eigen- Eigen-functions $\delta j_s^k(a)$ Eigen-functions $\delta j_p^k(a)$ values w_k ($N_J=6$, $N_P=4$) as functions of a .

Perturbations with $k > 9$ are invisible on B , j_p cannot be reconstructed

Slant ST plasma with $R/a=1.4$. Pressure profile is specified.



Logarithm of eigen- Eigen-functions $\delta j_s^k(a)$ Eigen-functions $\delta j_p^k(a)$ values w_k ($N_J=9$, $N_P=0$) as functions of a .

Perturbations with $k > 7$ are invisible on B

3 Summary

The practical technique for assessing the variances in equilibrium current density reconstruction was demonstrated

It can be used as routine post-equilibrium reconstruction processing.

The approach is open for insertion of other signals. (E.g., the diamagnetic signal should be included).

Kinetic measurements of pressure or MSE (or equivalents)

are crucial for equilibrium reconstruction